Weathering-Induced Strength Degradation and Hydro-Mechanical Controls on the Stability of Multilayered Tropical Rock Slopes

Luna, Stephanie Ivy
Department of Earth Resources Engineering, Kyushu University

Shimada, Hideki
Department of Earth Resources Engineering, Kyushu University

Sasaoka, Takashi
Department of Earth Resources Engineering, Kyushu University

Hamanaka, Akihiro
Department of Earth Resources Engineering, Kyushu University

https://hdl.handle.net/2324/7439375

出版情報：Journal of the Civil Engineering Forum. 12 (3), pp.415-424, 2026-08-05. Universitas Gadjah Mada
バージョン：

Journal of the Civil Engineering Forum, September 2026, 12(3):415-424
DOI 10.22146/jcef.29189
Available Online at https://jurnal.ugm.ac.id/v3/jcef/issue/archive

Weathering-Induced Strength Degradation and Hydro-Mechanical Controls on the Stability of Multilayered Tropical Rock Slopes

Stephanie Ivy Luna[1,2]*, Hideki Shimada[1], Takashi Sasaoka[1], Akihiro Hamanaka[1]
[1]Department of Earth Resources Engineering, Kyushu University, Fukuoka, JAPAN
[2]Mines and Geosciences Bureau Region III, Pampanga, PHILIPPINES
*Corresponding author: luna24r@mine.kyushu-u.ac.jp

SUBMITTED 3 March 2025 **REVISED** 23 May 2026 **ACCEPTED** 26 May 2026

ABSTRACT Tropical environments accelerate rock weathering, which can significantly reduce the stability of mineralized slopes. This study investigates the influence of weathering and groundwater conditions on the stability of a strong–weak–strong multilayered rock slope hosting an iron deposit in the Philippines, where intense rainfall and highly fractured rock masses are common. Detailed geological and hydrogeological investigations were conducted to construct two-dimensional numerical models of the slope system. Mechanical characterization of both weathered and unweathered rock masses was performed using field hardness testing and laboratory geomechanical tests. These parameters were incorporated into numerical simulations to evaluate slope stability under varying degrees of weathering, weak-layer thickness, and hydrological conditions derived from developed phreatic surfaces. Results indicate that when the middle weak layer is thin, a 50% weathering intensity still allows a stable multilayered slope at an Overall Slope Angle (OSA) of 60°. However, as weak-layer thickness increases, the same weathering degree leads to slope instability. Weathering effects recorded at the investigated study area correspond to an average reduction of 10.8 units in the Geological Strength Index (GSI), and are equivalent to a 50% weathering degree, implying that each 0.2 reduction in GSI represents approximately 1% weathering of the rock mass. Considering weathering-induced strength degradation, the optimally safe slope angle decreases from the originally designed 60° to approximately 35°, maintaining a minimum factor of safety of 1.2. Although the stabilizing effect of other countermeasures was excluded from this study. Hydrological analysis further reveals that low rainfall may temporarily increase slope stability due to matric suction induced by capillary effects in clay-like mineral sericite, although prolonged rainfall generates positive pore pressures that reduce stability. The thickness of the weak layer also produces localized increases in hydraulic gradient due to permeability contrasts, increasing susceptibility to rainfall-induced failure. These findings highlight the importance of quantitatively incorporating weathering and hydrogeological effects in slope design for tropical open-pit mines.

KEYWORDS weathering; multilayered slope; weak interlay; slope stability; volcanic-island arc setting; seepage-induced failure

1 INTRODUCTION

Tropical regions are characterized by persistently high temperatures, intense rainfall, strong monsoonal circulation, and frequent tropical cyclones. These climatic conditions significantly accelerate both mechanical and chemical weathering processes compared with temperate and arid environments. In tropical island arc settings such as Japan and the Philippines, the surrounding seas sustain a continuous hydrological cycle that maintains high atmospheric humidity and promotes prolonged water–rock interaction (Keller, 2021). Under such conditions, rock masses are subjected to rapid mineral alteration, dissolution, and structural weakening, which progressively reduce their engineering strength and durability (Fookes et al., 2000; Hencher, 2015). As a result, weathering plays a critical role in controlling the long-term stability of natural and engineered slopes in tropical terrains.

Previous studies have widely documented the influence of water infiltration on the degradation of soil and rock masses, particularly in relation to rainfall-induced landslides and rockfalls (Miscevi and Vlastelica, 2014; Shao et al., 2021; Rezaei and Mousavi, 2024). Rainfall infiltration increases pore-water pressure, reduces effective stress, and accelerates physicochemical alteration within rock discontinuities, all of which contribute to progressive slope instability (Erfen, 2017; Rahardjo, 2000). These processes are especially pronounced in fractured or altered rock masses where permeable discontinuities facilitate rapid water percolation. In mineralized terrains, the situation can become more critical because hydrothermal alteration and mineralogical heterogeneity often produce zones of reduced strength and increased susceptibility to weathering (Zhang et al., 2021). When such rock masses are excavated for mining or infrastructure development, the newly exposed surfaces are directly subjected to atmospheric agents, thereby accelerating weathering processes that were previously confined to subsurface conditions.

Excavated slopes in mineralized deposits are therefore particularly vulnerable to weathering-induced degradation. Mining operations commonly expose large rock faces, increasing the surface area available for interaction with rainfall, oxygen, and temperature fluctuations. Furthermore, mineralized rocks frequently exhibit intense fracturing associated with tectonic deformation and hydrothermal alteration. These fractures act as preferential pathways for water infiltration, enhancing chemical alteration and weakening the rock mass structure (Zhang et al., 2025). In many cases, such slopes consist of multiple lithological units with contrasting mechanical properties, forming complex stratified systems where failure mechanisms are controlled by the interaction between strong and weak layers. The presence of an intercalated weak layer within stronger rock units may create potential slip surfaces or localized deformation zones that significantly influence slope stability.

A representative example of such geological complexity can be observed in the excavated rock mass of a magnetite deposit in the Philippines. This deposit is one of the country's primary sources of iron ore and is characterized by a multilayered rock-mass structure, with relatively competent igneous rocks bounding weaker sedimentary or altered layers. Continuous excavation associated with mining operations exposes the rock mass to atmospheric conditions, promoting rapid weathering and increasing the likelihood of hydro-mechanically induced slope instability. Given the economic importance of such mineral resources and the potential hazards associated with slope failure, understanding the influence of weathering on slope behavior in these environments is of significant practical importance.

Although the role of weathering in modifying the engineering properties of soils and rocks has long been recognized, its systematic integration into slope stability analyses remains relatively limited. Many previous investigations have focused primarily on laboratory characterization of weathered materials or on rainfall-triggered landslides in natural slopes, while fewer studies have explicitly examined the progressive influence of weathering on engineered slopes such as those found in mining excavations or road cuts (Ersoz and Topal, 2018; Zhang et al., 2025). One possible reason for this limitation is the difficulty of translating qualitative field observations of weathering into quantitative parameters for incorporation into geotechnical models. Field classifications such as weathering grades, Geological Strength Index (GSI), or Rock Mass Rating (RMR) provide valuable descriptive information; however, converting these observations into mechanical parameters suitable for numerical modeling remains a challenge for many practitioners (Hoek and Carter, 2019).

Consequently, there remains a need for studies that bridge the gap between field-based weathering assessment and quantitative slope stability evaluation. In particular, limited research has systematically examined how varying degrees of weathering influence the hydro-mechanical response of multilayered rock slopes under different groundwater conditions. Moreover, the interaction between weathering-induced strength degradation and weak-layer configurations in layered rock masses has not been comprehensively analyzed using numerical modeling. Addressing this gap is essential for improving slope design strategies in tropical mining environments where weathering processes are particularly aggressive.

This study, therefore, aims to investigate the influence of weathering degree on the stability of a multilayer rock slope in a tropical mineralized environment. Specifically, the research seeks to (1) parameterize weathering phenomena observed in the field into quantifiable geotechnical properties, (2) compare the stability of weathered and unweathered slope conditions under both dry and saturated hydrogeological scenarios, (3) evaluate the hydro-mechanical behavior associated with different geometrical configuration of intercalated weak layer within stronger rock units due to changing slope design, and (4) determine an optimally safe slope angle for excavation design. By integrating field observations, rock mass characterization, and numerical slope stability modeling, the study provides a framework for translating weathering assessments into engineering design parameters. The findings are expected to contribute to improved understanding of weathering-controlled slope behavior in tropical mining environments and to support safer and more reliable slope design practices in similar geological settings.

2 METHODS

2.1 Research Design

After reviewing relevant literature and conducting a reconnaissance survey of the study area, a systematic research workflow was developed to address the study's objectives. The overall research procedure is illustrated in Figure 1. The study combined qualitative geological observations, quantitative data collection, and numerical modeling to evaluate the influence of weathering on the stability of an excavated multilayer rock slope.

The research adopted an integrated approach consisting of field investigation, laboratory testing, parameter estimation, and numerical slope stability analysis. Field investigations were conducted to characterize lithology, structural conditions, and degrees of weathering within the excavated rock mass. Quantitative data were obtained through rock hardness testing and limited laboratory testing of collected samples. This

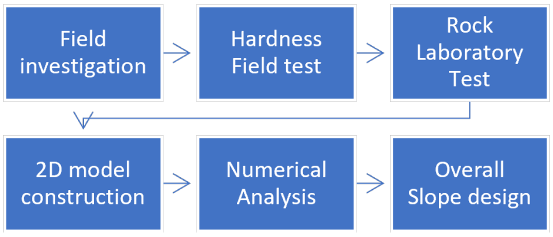

Figure 1. Activity flow chart.

data was subsequently used to estimate the mechanical parameters required for numerical slope modeling. The resulting models were then used to simulate various weathering and hydrogeological scenarios to evaluate their influence on slope stability.

Slope stability analysis was performed using the finite element software RS2. The Finite Element Method (FEM) was selected because it is well suited for analyzing complex geological systems and heterogeneous rock masses where stress–strain behavior varies spatially within the slope (Lim et al., 2016; Nata et al., 2024). Weathered rock masses often behave as quasi-continuous media due to fractures, alteration zones, and material degradation. The FEM approach, therefore, provides a more realistic representation of stress redistribution and deformation than traditional limit-equilibrium methods for heterogeneous rock slopes.

Slope stability was evaluated using the Shear Strength Reduction (SSR) technique, a widely used approach in finite element slope stability analyses. In this method, the shear strength parameters of the material are progressively reduced until failure occurs, and the reduction factor corresponding to failure is interpreted as the factor of safety (Harma et al., 2005; Hosseini et al., 2024). This technique was selected because it enables simultaneous evaluation of slope deformation and failure mechanisms while considering the stress–strain behavior of the rock mass.

Weathering processes in rock slopes are commonly associated with water–rock interactions that promote chemical alteration, mineral dissolution, and physical disintegration. Water infiltration through fractures and discontinuities may increase pore-water pressure and reduce effective stress, thereby decreasing the shear strength of the rock mass (Viles, 2012; Wyllie and Mah, 2017). To account for these hydro-mechanical interactions, the numerical simulations incorporated seepage conditions representing rainfall infiltration scenarios. The resulting changes in effective stress were evaluated using the SSR method to determine the corresponding slope stability factors.

The rock mass strength parameters required for the numerical analysis were estimated using the empirical Hoek–Brown failure criterion, which is widely applied in rock engineering practice for estimating rock mass strength from field-based observations and laboratory test results (Hoek and Brown, 2019). The parameters were derived based on lithological characteristics, estimated Uniaxial Compressive Strength (UCS), and Geological Strength Index (GSI) values obtained during field assessment.

The investigated slope had an overall height of approximately 40 m and consisted of a multilayered rock sequence with a hard–weak–hard configuration. From top to bottom, the slope was composed of basalt, sandstone/siltstone, and andesite units.

It is widely recognized that there is a higher safety risk of having a weak rock member in a heterogeneous slope than in a slope composed solely of hard rock (Díaz-Durán, 2023). For this reason, two thicknesses of the middle weak layer are extracted from the open pit and simplified for numerical modeling to assess the effect of varying the thickness of the weak middle layer. The two models considered middle-layer thicknesses of 5 m and 25 m, both dipping at $30°$ and positioned approximately 10 m above the pit bottom. Each geometric configuration was initially modeled with an Overall Slope Angle (OSA) of 60°.

Both geometric models were analyzed under two material conditions: fresh rock and weathered rock. This approach enabled comparison of the stability behavior between unweathered and weathered slope conditions. The results were subsequently used to identify an optimal slope configuration capable of maintaining stability under extreme rainfall conditions.

Obtaining sufficient undisturbed rock samples for laboratory testing in fractured rock masses can be difficult and costly. Therefore, representative sampling was complemented by extensive rock hardness testing using a Schmidt Hammer L-type. More than 100 rebound measurements were collected from both freshly excavated rock surfaces and older exposed slope faces. The Schmidt hammer method is widely used as a rapid and non-destructive technique for estimating the compressive strength of rock materials in the field (Aydin and Basu, 2005). The relative hardness reduction was calculated, representing the mechanical degradation inferred from field measurements. The reduction ratio was applied to the intact rock UCS to derive the equivalent weathered UCS.

The equivalent UCS values for fresh and weathered rock units are summarized in Table 1. The results indicated that weathering had caused substantial reductions in rock strength, particularly within the upper and middle layers of the slope. On average, the overall rock mass experienced approximately 49.78% strength reduction due to weathering processes. In addition, the average absolute deviation of 1.8 for the raw UCS data indicates a nearly uniform weathering rate across the rock mass layers exposed along the slope face.

Table 1. UCS equivalent of weathered and unweathered rock members

Rock Members	Fresh Rock σ_c	Weathered Rock σ_c	% Weathering
Top Layer (TL)	90 MPa	34.43 MPa	61.74%
Middle Layer (ML)	60 MPa	22.50 MPa	62.50%
Bottom Layer (BL)	100 MPa	74.89 MPa	25.11%
Average Overall Slope Weathering			49.78%

In addition to strength estimation, the overall rock mass quality was evaluated using the Geological Strength Index (GSI) classification system. The GSI method provides a practical means of characterizing rock mass structure and surface conditions based on visual field observations (Hoek and Carter, 2019). Fresh and weathered slope conditions were visually assessed using the GSI chart, and the corresponding values for each rock unit are summarized in Table 2.

Table 2. GSI equivalent of weathered and unweathered rock members

Rock Members	Fresh GSI	Weathered GSI	Unit Reduction
TL	60	47	13
ML	30	20	10
BL	80	70	10
Average Overall GSI Reduction			11

Because weathering intensity may vary spatially and temporally depending on environmental exposure (Babaei et al., 2020), the equivalent GSI values used in the numerical simulations were calibrated through back-calculation until exactly the same Factor of Safety was obtained to that weathered by UCS model allowing for theoretically zero margin of error. Specifically, the factor of safety obtained from simulations using reduced UCS values was compared with results obtained from simulations using reduced GSI values. Through trial-and-error adjustment, equivalent parameter reductions were identified when both approaches produced similar stability factors. During this calibration process, only one parameter was modified at a time in order to avoid altering the fundamental rock type represented in the model.

This procedure was used to represent different mechanisms of weathering-induced deterioration within the rock mass. Reductions in UCS were interpreted to primarily reflect chemical weathering, which weakens the intact rock material through mineral alteration. In contrast, reductions in GSI were interpreted to represent physical weathering, characterized by increased fracturing and structural degradation of the rock mass. By combining these two approaches, the numerical models were able to simulate the progressive deterioration of the same rock mass under varying degrees of weathering.

3 RESULTS

3.1 Weathering Characterization of Multilayered Slope

Field observations indicated that the investigated slope had already undergone substantial weathering at the time of investigation. Based on rock mass assessment and parameter calibration, the overall slope condition corresponded to approximately 50% weathering, which was represented by an 11-unit reduction in Geological Strength Index (GSI). This corresponds to an approximate 4.7% weathering deterioration per unit reduction in GSI.

The weathering parameters used in the numerical simulations are summarized in Table 3. The parameters were defined by comparing chemically weathered and physically weathered conditions using equivalent reductions in uniaxial compressive strength (σ_c) and GSI values. The parameter sets produced identical stability results for both slope sections.

Table 3. Parametrized weathered conditions of two slope sections for GSI rating verification

Rock Members	Chemically Weathered		Physically Weathered	
Parameter	σ_c	GSI	σ_c	GSI
TL	34.43	60	90	47
ML	22.50	30	60	20
BL	74.89	80	100	70
Identically obtained	1.2 (slope cut section 1)			
Factor of Safety	0.93 (slope cut section 2)			
Weathering %	50%			
GSI Reduction	11			

The results showed that the top layer (TL) experienced slightly higher reduction in GSI than the weak middle layer (ML), despite having higher intact rock strength. It is hypothesized that the orogenic stage of mineralization influenced the later-stage fracturing of the brittle, hard rock above (TL), while the more plastic middle weak rock (ML) absorbed external stress through deformation (Díaz-Durán, 2023; Fookes et al., 2000). The initial fracturing condition of TL resulted in a higher void ratio, which allows for larger accommodation of transient waters that drive the weathering process. The field photographs used for the GSI evaluation are presented in Figure 2, which illustrates the differences between unweathered and weathered rock-mass conditions for each lithological layer.

Table 3 shows that the estimated UCS values for the

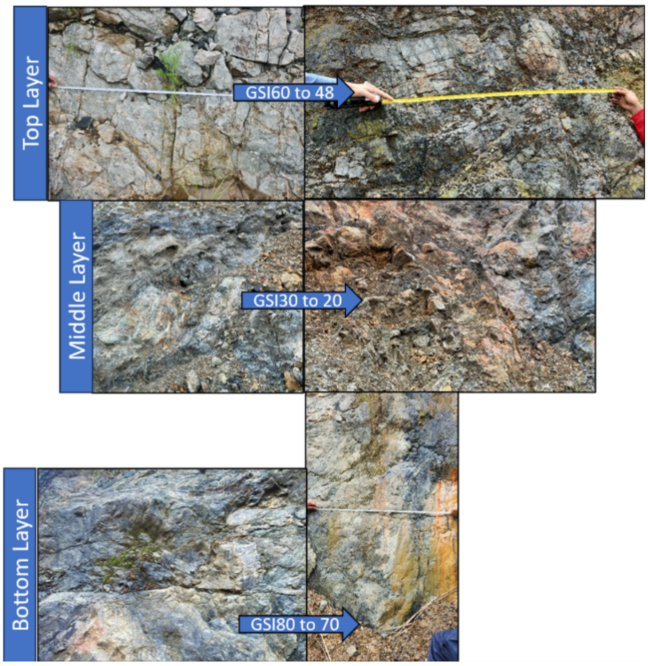

Figure 2. Geological Strength Index (GSI) ratings of unweathered (left column) and weathered (right column) rock masses for each stratigraphic layer (from top to bottom).

weathered condition were 34.43 MPa, 22.5 MPa, and 74.89 MPa for the top, middle, and bottom layers, respectively. In contrast, the corresponding UCS values for the fresh rock condition were 90 MPa, 60 MPa, and 100 MPa. The equivalent GSI values for the weathered condition were 47, 20, and 70, compared with 60, 30, and 80 for the fresh rock mass.

The calibrated parameter sets resulted in identical factors of safety for both slope sections, with $FS = 1.20$ for slope cut section 1 and $FS = 0.93$ for slope cut section 2.

3.2 Stability Behavior at Varying Weak Middle Layer Thickness under Dry and Wet Conditions

The two slope sections extracted here are distinguished by their difference in thickness of the Weak Middle Layer (MWL). Model 1 represented a 5 m thick weak layer, while Model 2 represented a 25 m thick weak layer of the actual measured thickness at the two most active slope sections at the mine site. Both models were analyzed under fresh and weathered rock conditions and under dry and rainfall scenarios.

The calculated factors of safety for these scenarios are presented in Table 4. Under dry conditions, Model 1 produced factors of safety of 1.74 for the fresh slope and 1.20 for the weathered slope. Model 2 produced factors of safety of 1.35 for the fresh slope and 0.93 for the weathered slope.

Under wet conditions representing high rainfall, the

Table 4. Factor of safety of two slope sections at different weather conditions

	Dry Condition		Wet Condition (High Rainfall)	
Slope Models	Fresh Slope	Weathered Slope	Fresh Slope	Weathered Slope
Model 1	1.74	1.20	1.34	0.93
Model 2	1.35	0.93	0.80	0.71

calculated factors of safety decreased for both models. Model 1 produced factors of safety of 1.34 for the fresh slope and 0.93 for its weathered condition. Model 2 produced factors of safety of 0.80 for the fresh slope, while the effect of weathering reduced its factor of safety to 0.71. Under dry conditions, the safety factor reduction between the fresh and weathered versions of the slope mass is 0.54 and 0.42 for Model 1 and Model 2, respectively. During heavy rain, the reduction became 0.41 and 0.48, respectively.

The models were initially analyzed with an overall slope angle (OSA) of 60°. The results indicated variations in stability between the two slope models and weathering conditions.

Additional simulations were conducted to evaluate the effect of different rainfall intensities on the fresh slope condition. The rainfall intensities are based on actual rain gauge data in the area, with four intensities selected based on the worst-case quartile scenario (peak-per-quartile). The resulting factors of safety are summarized in Table 5, excluding the rare extreme conditions reserved for the worst-case envelope after final design is established. For Model 1, the calculated FS values were 1.74 under dry conditions, 1.84 under low rainfall, 1.47 under moderate rainfall, and 1.34 under high rainfall. For Model 2, the corresponding FS values were 1.35, 0.79, 0.79, and 0.80, respectively.

Table 5. Factor of safety of the fresh slope at 60° OSA under different rainfall intensities

	Dry	Low	Moderate	High
Model 1	1.74	1.84	1.47	1.34
Model 2	1.35	0.79	0.79	0.80

The results indicated that the factor of safety varied with rainfall intensity and differed between the two slope models.

3.3 Stability Performance at Different OSA

Additional simulations were performed to evaluate the effect of different Overall Slope Angles (OSAs) on slope stability. The analysis was conducted using weathered Model 2 under dry conditions since it is the section

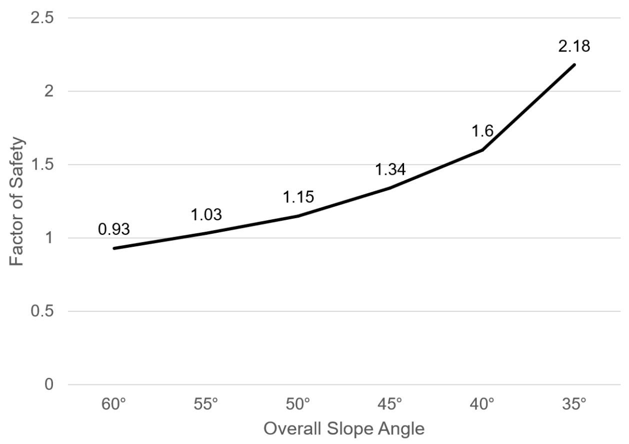

Figure 3. Factor of safety of Weathered Model 2 under different slope angles.

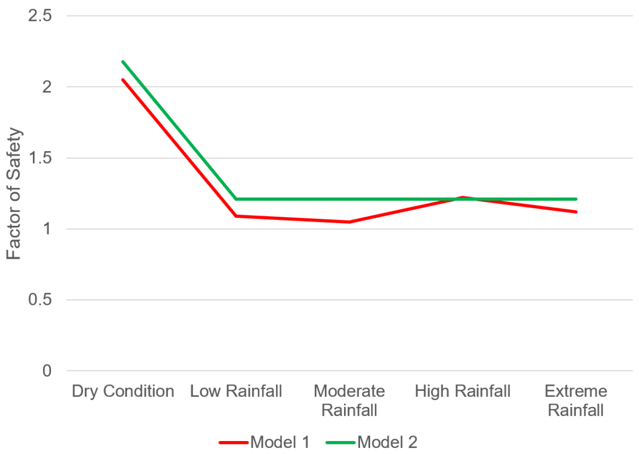

Figure 4. Stability performance of the 35° optimum slope angle (OSA) under different rainfall intensities for Weathered Models 1 and 2.

with the critical factor of safety (Wightman and Norris, 2025), and the OSA was systematically reduced from the initial 60°.

The calculated factors of safety for the different slope angles are presented in Figure 3. The results showed an increase in the factor of safety as the slope angle decreased. The relationship between slope angle and factor of safety showed a strong correlation with a coefficient of determination $R^2 = 0.95$.

Based on these results, an OSA of 35° was selected for further evaluation. Both weathered slope models were subsequently analyzed at this slope angle under varying rainfall intensities, including a fourth category representing a rare extreme rainfall event associated with a 100-year return period in the study area. This additional rainfall scenario was incorporated to evaluate the final slope configuration under worst-case conditions and to account for the possibility of such an extreme event occurring in the future. The resulting stability performance is shown in Figure 4.

The calculated factors of safety at 35° OSA remained above the stability threshold across the simulated rainfall scenarios for both models. The results also showed variations in FS values between dry conditions and rainfall conditions, as illustrated in Figure 4.

4 DISCUSSION

The results demonstrated that the parameterization technique used to represent weathering through both Uniaxial Compressive Strength (UCS) reduction and Geological Strength Index (GSI) reduction produced identical factors of safety for two independent slope sections. This outcome confirms that the approach adequately represents the combined effects of chemical and mechanical weathering processes acting on the rock mass. Chemical weathering processes such as hydrolysis, oxidation, and dissolution alter the internal structure of rocks, resulting in increased porosity, destruction of cementation, and mineral transformation, all of which significantly lower the rock's load-bearing capacity (Hasan et al., 2024). This puts Uniaxial Compressive Strength (UCS) as a key indicator and direct consequence of chemical weathering. On the other hand, GSI is used to estimate rock mass strength and deformation by evaluating two main components: rock structure (blockiness) and joint surface conditions. Physical weathering directly impacts these components, reducing the overall GSI value (Berisavljević et al., 2018). Although in natural environments, weathering rarely occurs as a single, isolated mechanism; instead, chemical alteration and mechanical disintegration occur simultaneously as a result of water–rock interaction and environmental exposure. Representing weathering through both strength and structural degradation, therefore, provides a practical method for simulating weathered rock masses in slope stability analyses. Similar approaches have been adopted in rock engineering studies where rock mass deterioration is represented through reductions in intact strength and rock mass quality parameters (Hoek and Carter, 2019; Wyllie and Mah, 2017).

The results also showed that the stability of the multilayered slope strongly depended on the thickness of the weak middle layer. At an Overall Slope Angle (OSA) of 60°, the weathered slope containing a thick weak interlayer (Model 2) reached instability even under dry conditions. In contrast, the slope containing a thin weak interlayer (Model 1) remained stable under dry conditions but approached instability when subjected to high rainfall conditions. These results indicate that the geometry of the weak layer plays a major role in controlling slope behavior in multilayer rock masses. Similar observations have been reported in studies of heterogeneous rock slopes where weak interbeds govern the location and development of failure surfaces (Díaz-Durán, 2023).

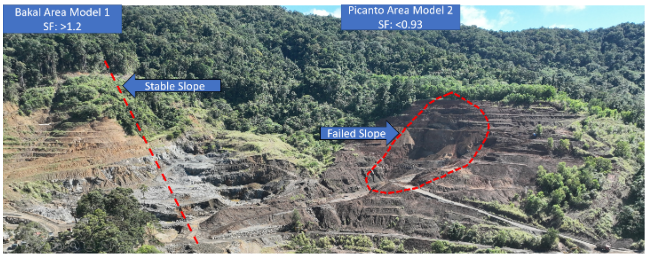

Figure 5. Photographs of a stable slope (left side) and a failed slope (right side) in the study area.

Field observations provided additional support for the modeling results. At the time of the site visit, the slope had already experienced approximately 50% weathering, equivalent to a reduction of 10–11 units in GSI. The observed slope conditions, as shown in the photograph in Figure 5, corresponded with the stability predictions from the numerical models. The section represented by Model 1 was observed to remain stable at an approximate slope angle of 45°, while the section represented by Model 2 had already experienced failure at a slope angle approaching 80°. The slope condition shown in the actual photographs in Figure 5 verifies that the constituted model, within its assumptions, is not just a theoretical simulation but accurately mirrors the current site condition. Model 1 was tested at 60°, so it is projected that the slope should continue to stand at 45°. On the other hand, Model 2 stability status was demonstrated using the same 60°, so intuitively, a slope higher than 60°, which 60° already resulted in $FS < 1$, will surely result in anticipated failure. These observations support the relationship between weak-layer thickness and slope stability identified in the numerical simulations.

The difference of the derived factor of safety between weathered and unweathered models is in the order of 0.4 to 0.5 units. By rule-of-thumb from experience, the 1st decimal number of the factor of safety is already a significant number to indicate the magnitude of stability, so a 0.5 unit decrease indicates 50% change to the stability status of the slope, which is already a major change in the fate of the slope. This is aggravated by changes in weak-layer thickness. This shows that weathering plays a major role in dictating the slope's risk level, especially when it occurs in a weak rock type.

The parametric analysis of overall slope angles further demonstrated that slope stability was highly sensitive to geometric configuration in multilayer rock masses. The results showed that decreasing the slope angle produced an exponential increase in the factor of safety, indicating a strong dependence of stability on slope geometry. This behavior suggests that the weak interlayer is particularly sensitive to local steepness and to the layer's orientation relative to the slope face. Similar sensitivity of layered rock slopes to slope geometry has been documented in previous studies of stratified rock masses, where interlayer strength contrasts control failure mechanisms (Ma et al., 2025).

The analysis identified 35° as the steepest slope angle capable of maintaining stability under the most extreme rainfall conditions simulated in this study. From a design perspective, this implies that slope instability associated with progressive weathering and tropical rainfall conditions may be mitigated by reducing the overall slope angle to this range. However, such geometric modification also implies additional excavation or waste movement during mining operations. This is a 25° of equivalent volume as addition to mine waste movement. But on the other perspective, the 25-unit gentler slope implies overcoming the risk associated with a 50% weathering degree. From an analytical point of view, that is a 2-unit angle reduction to address risk from just 1% degree of weathering or a 1% weathered level of the excavated rockmass. A 2-unit can be excessive effort for a very small effect in risk elimination. This signals that weathering plays an intense role in slope design. The results, therefore, highlight the strong influence of weathering on slope design in tropical mining environments. Even moderate levels of weathering can require significant geometric adjustments to maintain acceptable stability conditions, especially when the slope is expected to be saturated from continuous rainfall.

The results also revealed differences in failure behavior between the two slope models under rainfall conditions, as illustrated in Figure 6. For the slope containing a thin, weak interlayer (Model 1), rainfall primarily produced localized instability mechanisms associated with tensile failure and small rockfalls in the upper hard-rock layer. In contrast, the slope containing a thick weak interlayer (Model 2) exhibited composite shear failure concentrated within the weak layer. In both cases, however, the simulated failure surfaces remained confined within the boundaries of the weak interlayer and did not propagate into the lower hard-rock layer. This indicates that the weak interlayer acted as the dominant mechanical control on slope failure in the investigated multilayer configuration. However, the model developed only involved a single weak layer that has participated in the excavated slope. A repeated sequence of weak layers might behave differently, which is beyond the scope of this study. Nevertheless, it is established that the preferential failure plane will always involve or be located among the weak zones.

Hydro-mechanical responses of the slope models also varied depending on rainfall intensity. For unweathered Model 1, a temporary increase in the factor of safety was observed immediately after the onset of low rainfall (Table 5 and Figure 7b). Examination of the simulated pore-water pressure distribution indicated that this response corresponded with the development of negative pore-water pressure (matric suction) within

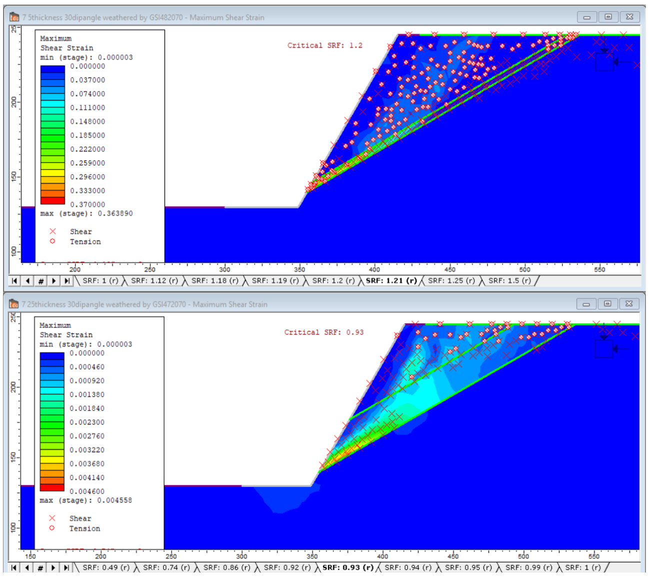

Figure 6. Deformation strain and corresponding failure mode for (a) Weathered Model 1 and (b) Weathered Model 2.

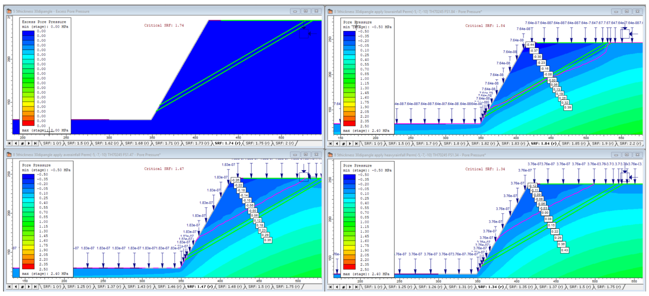

Figure 7. Pore pressure distribution under different weather conditions for Unweathered Model 1: (a) dry, (b) low rainfall, (c) moderate rainfall, and (d) heavy rainfall.

the partially saturated rock mass (Lu, 2020), as shown in Figure 7. Negative pore pressure increases effective stress within the rock mass and therefore provides temporary mechanical stabilization. This behavior is consistent with the Soil–Water Characteristic Curve (SWCC) applied in the seepage model, which reflects the hydraulic properties of the clay-rich alteration minerals associated with the magnetite deposit.

At higher rainfall intensities, however, the phreatic surface rose more rapidly and eventually intersected the weak interlayer, as illustrated in Figure 8. Once the weak layer became saturated, the stabilizing effect of matric suction diminished, and the factor of safety began to decrease. The phenomena suggest that the slow movement of water percolation from the onset of rainfall dissipates pressure through the capillary effect of these alteration minerals, predominantly sericites, which bind the grains together (Figure 7). This resulted in a phreatic surface found below the middle weak layer, thereby not activating the impact of the weak layer on overall stability. But as infiltration accelerates, the rapid rise of the phreatic surface surpasses

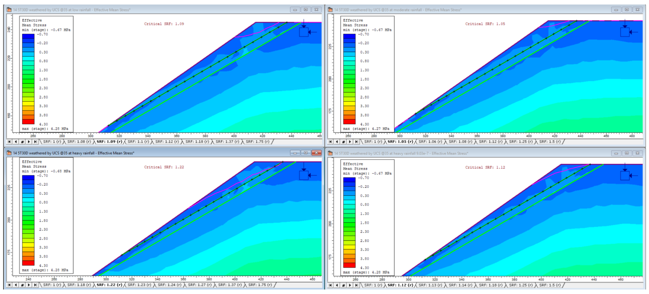

Figure 8. Effective stress contours of Weathered Model 1 under different rainfall scenarios: (a) low rainfall, (b) moderate rainfall, (c) heavy rainfall, and (d) extreme rainfall.

the weak interlayer zone (Figure 8), where the weak layer finally reacts to overall slope stability, giving the usual downtrend in the Factor of Safety.

As shown in Figure 4, there appears to be a slight local increase in FS from low jump to high rainfall in the weathered Model 1. Influx rate at the onset of rainfall, with respect to the infiltration capability of the fractured rock medium, was given enough time to seep through the middle weak-layer zone, reacting most of the seepage force to the most vulnerable layer of the slope, thereby affecting the overall stability. The simulated phreatic surface geometry reflected this transition. At low infiltration rates, the phreatic surface developed a concave configuration (Figure 8a–b), indicating a gradual buildup of pore pressure within the interior of the slope. Under higher infiltration rates, the phreatic surface became convex, reflecting rapid pore-pressure accumulation and drainage within the shallow rock layers (Figure 8c–d). With higher rainfall, the increased seepage influx caused the seepage vector to reroute immediately at the shallow hardrock layer, resulting in high displacement, but it does not affect the overall stability of the slope, since the movement occurs only within a small, shallow radius.

In the weathered slope containing a thick, weak interlayer (Model 2), the hydro-mechanical response differed from that of weathered Model 1. The factor of safety remained nearly constant despite increasing rainfall intensity because the weak layer in Model 2 saturated almost immediately after rainfall began. Numerical results (Figure 9) show rapid convergence during early load steps, indicating early full saturation. Once saturated, the weak layer had already reached its critical mechanical condition, so additional rainfall did not further reduce slope stability.

Finally, the results showed that at 35° OSA, both slope models produced nearly identical factors of safety across different weather and rainfall scenarios (Figure 4). This convergence in stability behavior appears to result from the increasing exposure of the weak interlayer along the slope face as the slope becomes gentler. At lower slope angles, a larger proportion of the

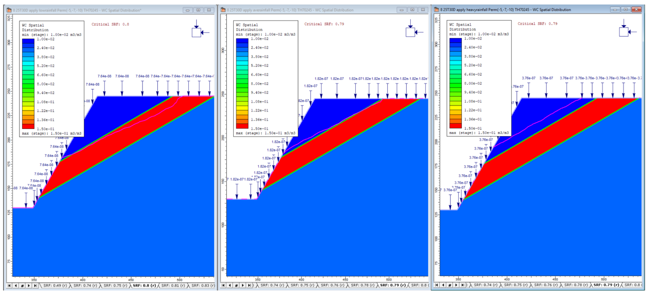

Figure 9. Spatial distribution of water content in Weathered Model 2 under different rainfall intensities: (a) low rainfall, (b) moderate rainfall, and (c) heavy rainfall.

slope surface is composed of the weak layer, allowing it to dominate the slope's overall mechanical response, regardless of its original thickness. This suggests that there may exist a threshold exposure of the weak layer beyond which its thickness no longer significantly influences overall slope stability.

Overall, the study provides new insight into how weathering, weak-layer thickness, and rainfall infiltration interact to control the stability of multilayer rock slopes in tropical mining environments. The results emphasize that slope design in such environments must consider both the progressive deterioration of rock mass properties due to weathering and the hydro-mechanical effects associated with intense rainfall events.

5 CONCLUSSION

This study investigated how weathering influences the hydro-mechanical stability of a multilayered rock slope representative of tropical environments. The results confirmed that progressive weathering significantly reduced the stability performance of the slope, particularly under rainfall-induced saturation conditions that commonly occur in tropical climates. Lower factors of safety were generally associated with increased weathering degrees due to the reduction in rock mass strength and stiffness, although the analysis also demonstrated that slope response was not strictly linear. The presence of lithological heterogeneity introduced additional complexity, where parameters such as weak layer thickness, permeability contrasts, and the proportion of exposed weak material along the slope face influenced stability behavior. The findings further showed that weak rock units were sensitive to their geometric position within the overall slope configuration, indicating that structural arrangement plays a critical role in controlling failure susceptibility. From an engineering perspective, reducing the overall slope angle was shown to mitigate weathering-related instability, although the resulting safe slope geometries may not always be economically optimal for mining operations and therefore must be carefully considered during feasibility assessments. For infrastructure slopes such as road cuts, the results support the implementation of permanent stabilization measures that explicitly account for weathering-induced degradation. This study contributes to the existing literature by highlighting the combined influence of weathering progression and hydro-mechanical interactions in heterogeneous tropical rock slopes, an aspect that remains insufficiently quantified in many stability analyses. Nevertheless, the study was limited to numerical simulations based on representative material parameters and simplified geological configurations. Future research should incorporate detailed field monitoring, laboratory weathering characterization, and more complex geological models to further validate the observed non-linear stability responses and improve predictive approaches for tropical slope engineering.

DISCLAIMER

The authors declare no conflict of interest.

ACKNOWLEDGMENTS

The authors acknowledge the support program for advanced studies given by the Japan International Cooperative Agency. The authors also express gratitude to Ore Asia & Mining Development Corporation for granting site access.

REFERENCES

Aydin, A. and Basu, A. (2005), 'The schmidt hammer in rock material characterization', *Engineering Geology* **81**(1), 1–14.

Babaei, F. D. et al. (2020), 'Relating the spatial variability of chemical weathering and erosion to geological and topographical zones', *Geomorphology* **363**.

Berisavljević, Z., Berisavljević, D., Rakić, D. and Radić, Z. (2018), 'Application of geological strength index for characterization of weathering-induced failures', *Građevinar* **70**(10), 891–903.

Díaz-Durán, F. A. (2023), Slope stability in open pits with thin weak layers, *in* 'Atlantis Highlights in Engineering'.

Erfen, H. F. W. S. (2017), 'Effect of weathering grade on mechanical properties of rocks from ranau, sabah', *Earth Science Malaysia* **1**(2), 1–6.

Ersoz, T. and Topal, T. (2018), 'Weathering and excavation effects on the stability', *Geotechnical and Geological Engineering* **36**, 3707–3729.

Fookes, P. G., Baynes, F. J. and Hutchinson, J. N. (2000), Total geological history: A model approach to the anticipation, observation and understanding of site conditions, *in* 'Proceedings of the International Society for Rock Mechanics and Rock Engineering', Melbourne.

Harma, R. E., Yacoub, T. E., Corkum, B. C. and Curran, J. H. (2005), The shear strength reduction method for the generalized hoek–brown criterion, *in* 'American Rock Mechanics Association Conference', Anchorage.

Hasan, M. et al. (2024), 'Influence of rock weathering and saturation on compressive strength and slope stability: A uniaxial test analysis', *International Journal of Safety and Security Engineering* **14**(1), 145–153.

Hencher, S. (2015), *Practical Rock Mechanics*, 1 edn, CRC Press, Boca Raton.

Hoek, E. and Brown, E. T. (2019), 'The hoek–brown failure criterion and gsi – 2018 edition', *Journal of Rock Mechanics and Geotechnical Engineering* **11**(3), 445–463.

Hoek, E. and Carter, T. (2019), 'Practical considerations for estimating rock mass strength', *Rock Mechanics and Rock Engineering* **52**(2), 431–447.

Hosseini, S. S. et al. (2024), 'Investigation of shear strength reduction method in slope stability of reinforced slopes by anchor and nail', *Buildings* **14**(2).

Keller, E. A. (2021), *Introduction to Environmental Geology*, 5 edn, Pearson.

Lim, K., Li, A. J., Schmid, A. and Lyamin, A. V. (2016), 'Slope-stability assessments using finite-element limit-analysis methods', *International Journal of Geomechanics* **17**(2).

Lu, N. F. (2020), 'Unsaturated soil mechanics: Fundamental challenges, breakthroughs, and opportunities', *Journal of Geotechnical and Geoenvironmental Engineering* **146**(5).

Ma, L. et al. (2025), 'Failure mechanism of soft–hard interbedded rock slopes in cold regions: Numerical simulation and theoretical analysis', *PLoS ONE* **20**(3).

Miscevi, P. and Vlastelica, G. (2014), 'Impact of weathering on slope stability in soft rock mass', *Journal of Rock Mechanics and Geotechnical Engineering* **6**, 240–250.

Nata, R. A. et al. (2024), 'Finite element modeling for stability assessment of sedimentary', *Safety* **10**(70).

Rahardjo, H. (2000), 'Rainfall-induced slope failures'. Seminar/Technical Paper.

Rezaei, M. and Mousavi, S. Z. S. (2024), 'Slope stability analysis of an open pit mine with considering the weathering agent: Field, laboratory and numerical studies', *Engineering Geology* **333**.

Shao, K. S. et al. (2021), 'Investigations of a weathered and closely jointed rock slope failure using back analyses', *Sustainability* **13**(23).

Viles, H. A. (2012), 'Linking weathering and rock slope instability: Non-linear perspectives', *Earth Surface Processes and Landforms* **38**(1), 62–70.

Wightman, A. and Norris, N. (2025), Risk-based approach to factor of safety selection, Technical report, Unknown.

Wyllie, D. C. and Mah, C. W. (2017), *Rock Slope Engineering*, 5 edn, Taylor and Francis Group, Boca Raton.

Zhang, S. et al. (2025), 'Stability influence of weak interlayer rock slope under rainfall', *Frontiers in Earth Science* **13**, 1–13.

Zhang, Z. et al. (2021), 'Deterioration of physical and mechanical properties of rocks by cyclic drying and wetting', *Geofluids* **2021**(1).